Atmospheric
Chemistry
and Physics

Supplement of

Organosulfate produced from consumption of SO_3 speeds up sulfuric acid–dimethylamine atmospheric nucleation

Xiaomeng Zhang et al.

Correspondence to: Shi Yin (yinshi@m.scnu.edu.cn)

Supporting information

Table of contents

Supporting information

Selection of simulated box and boundary clusters

For H_2SO_4-DMA system, "3 × 3" box has always been adopted in previous studies (Liu et al., 2021). The box for the H_2SO_4-DMA-based system is set to the size of "3 × 3" to contain the $(GA)_x(SA)_y(DMA)_z$, $(GAS)_x(SA)_y(DMA)_z$, and $(GAS)_x(SA)_y(DMA)_z$ ($0 \leq z \leq x + y \leq 3$) clusters.

In the process of cluster growth, the stability of cluster can be judged by the competition between evaporation into smaller clusters or collision. The collision rate constant of a cluster with acid or base monomer is of the order of 10^{-10} cm^3 s^{-1}, and the collision rate can be considered to be about 10^{-2} s^{-1} under the condition of base/acid monomers at ppt level. Thus, the cluster can be considered to be stable enough when the collision rate is higher than that of evaporation, and a given cluster can be deemed as stable enough for further growth when the evaporation rate is lower than 10^{-3} s^{-1}.

The boundary clusters are allowed to leave the simulation box for further growth, which means the boundary clusters are needed to be stable enough and have the potential to continue growing. Furthermore, generally speaking, the clusters with approximately equal numbers of acidic molecules and base molecules or number of acidic molecules one greater than that of base molecules are assumed to have the potential for further growth. Hence, only clusters that satisfy the above conditions are calculated.

As shown in Figure S3, the evaporation rates for all glycolic acid (GA)-involved clusters has been predicted to be higher than 10^1 s^{-1}. Therefore, the boundary clusters are $(SA)_4(SA)_3$ and $(SA)_4(SA)_4$ clusters for GA-SA-DMA system. As for GAS-SA-DMA system, the $(GAS)_3(DMA)_3$, $(GAS)_2(DMA)_2$, and $(GAS)_1(SA)_2(DMA)_3$ clusters are stable enough against evaporation. Thus, $(GAS)_4(DMA)_3$, $(GAS)_4(DMA)_4$, $(GAS)_2(SA)_2(DMA)_3$, $(GAS)_2(SA)_2(DMA)_4$, $(GAS)_3(SA)_1(DMA)_3$, $(GAS)_3(SA)_1(DMA)_4$, $(GAS)_1(SA)_3(DMA)_3$, $(GAS)_1(SA)_3(DMA)_4$, $(SA)_4(SA)_3$ and $(SA)_4(SA)_4$ clusters are acting as boundary clusters for GSA-SA-DMA system. Similarly, the $(GASA)_4(DMA)_3$, $(GASA)_4(DMA)_4$, $(GASA)_2(SA)_2(DMA)_3$, $(GASA)_2(SA)_2(DMA)_4$, $(GASA)_3(SA)_1(DMA)_3$, $(GASA)_3(SA)_1(DMA)_4$, $(GASA)_1(SA)_3(DMA)_3$, $(GASA)_1(SA)_3(DMA)_4$, $(SA)_4(SA)_3$ and $(SA)_4(SA)_4$ clusters are defined as boundary clusters for GASA-SA-DMA system for the reason that $(GASA)_3(DMA)_3$, $(GASA)_2(DMA)_2$, and $(GASA)_1(SA)_2(DMA)_3$ clusters are stable enough against evaporation.

Supporting information

Kerminen−Kulmala equation

According to the revised Kerminen−Kulmala equation (Anttila et al., 2010;Lehtinen et al., 2007), cluster formation rates for 3.0 nm clusters ($J_{3.0}$) relate to those for 1.3 nm clusters ($J_{1.3}$) by

$$J_x = J_1 \cdot \exp[-\gamma \cdot d_1 \cdot \frac{CS(d_1)}{GR}]$$

$$\gamma = \frac{1}{m+1}[(\frac{d_x}{d_1})^{m+1} - 1]$$

where GR is the initial cluster growth rate from 1.0 to 3.0 nm, CS represents condensation sink of clusters by preexisting particles and γ is calculated as the function of d. For typical atmospheric aerosols, the value of m can be set to -1.9. If we choose d_1 = 1.3 nm, d_x = 3 nm, so that $J_{1.3}$ corresponds to the "nucleation rate" at 1.3 nm and J_3 to the "nucleation rate" at 3 nm, and set m = -1.9 corresponding to typical Hyytiälä event-day conditions, we have $\gamma \approx 0.5$. GR was measured to be 3.1 nm·h^{-1} for 3.0 nm size particles during the observed events (Riipinen et al., 2007). The coagulation sink in Hyytiälä is at the level of 10^{-3} s^{-1} (Olenius et al., 2013; Dal Maso et al., 2008). Thus we can roughly get the approximate relationship $J_3 \approx 0.5\ J_{1.3}$.
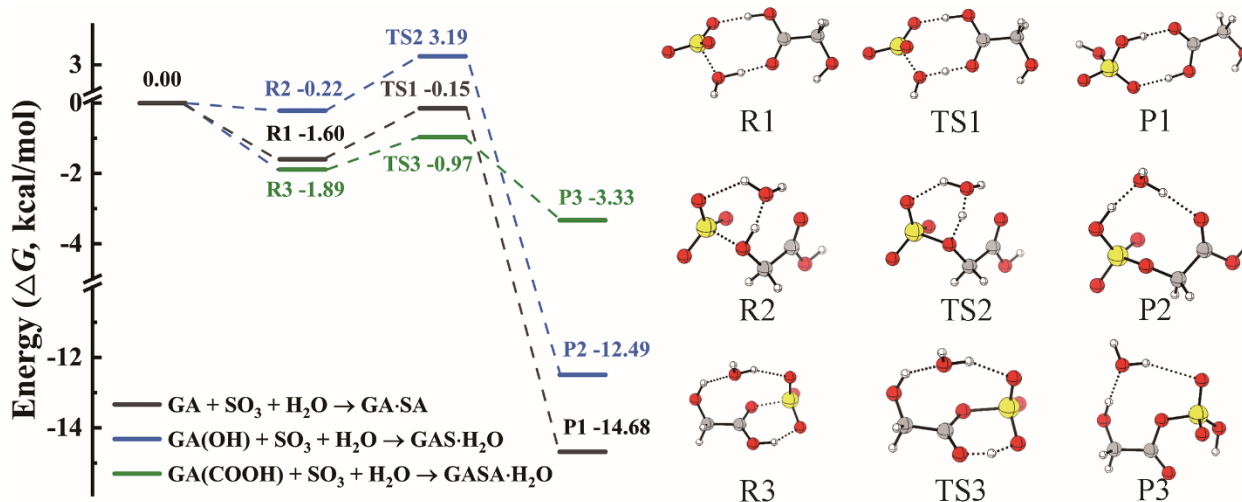
Supporting information

Figure S1. Potential energy surfaces at the DLPNO-CCSD(T)/aug-cc-pVTZ//M06-2X/6-311++G(3df,3pd) level of theory in units of kcal mol^{-1} (at 298 K, 1atm) for the gas-phase reaction of GA, SO$_3$ and H$_2$O. The green line represents the pathway through SO$_3$ attacking the -OH group of GA with H$_2$O as a catalyst; the blue one represents the SO$_3$ attacking the -COOH group of GA pathway with H$_2$O as a catalyst; and black one represents the pathway to form H$_2$SO$_4$ with H$_2$O as a catalyst. R, TS, and P refer to pre-reaction complex, transition state, and product, respectively. Hydrogen, carbon, oxygen, and sulfur atoms are represented by white, gray, red, and yellow spheres, respectively.

Related discussions

The -COOH group of GA and -S=O from SO$_3$ can form six-membered ring in transition state rather than closed four-membered ring. Meanwhile, according to the Electrostatic potential (ESP) on molecular van der Waals (vdW) surface of GA and SO$_3$ molecules from our previous study (Tan et al., 2022), the sulfur atom in the SO$_3$ molecule possesses more positive ESP and the oxygen atoms of -COOH/-OH group possesses more negative ESP, making both of the two pathways for GA-SO$_3$ reaction feasible to occur. Also, the oxygen atoms of SO$_3$ molecule possess relatively negative ESP, which could interact with the hydrogen atoms of -COOH/-OH group. Therefore, the gas-phase reaction between GA and SO$_3$ is feasible to occur. Furthermore, the SO$_3$-H$_2$O reaction, which is commonly recognized as important loss process of SO$_3$, could be catalyzed by GA. Although H$_2$O will be dominant sink pathway for SO$_3$, GA-SO$_3$ can be comparable to that of SO$_3$-H$_2$O in highly polluted areas with relatively dry and cold conditions. The gaseous concentration of H$_2$O is drastically reduced at lower temperature and dry condition (Renard et al., 2004). Hence, the GA-SO$_3$ reaction may compete with the hydration reaction of SO$_3$.
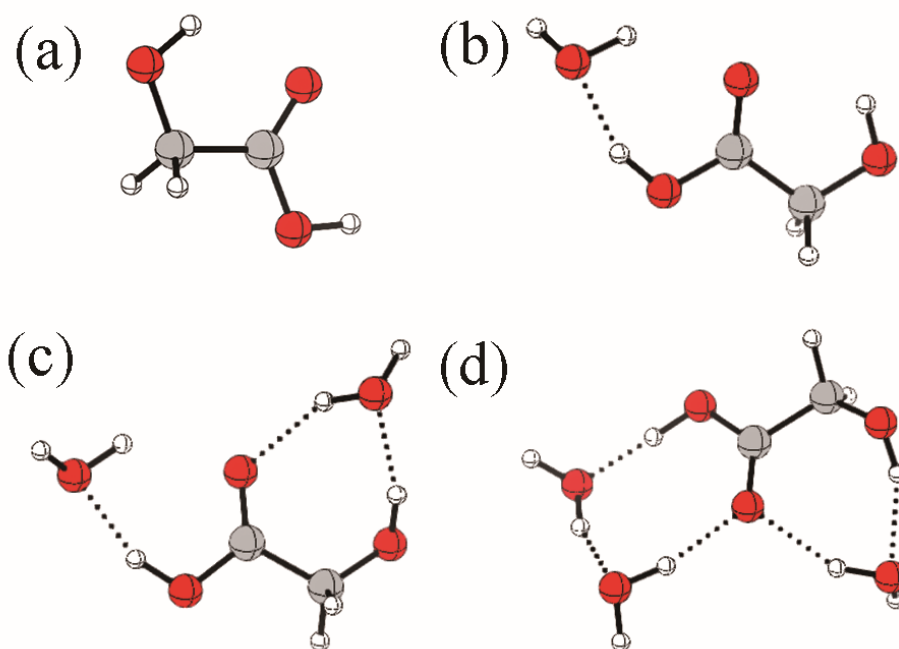
Figure S2. Lowest energy geometries of (GA)(H$_2$O)n, optimized with the M06-2X/6-311++G(3df,3pd) method. The color coding is red for oxygen, grey for carbon, and white for hydrogen. The number of water molecules increases from (a) where n = 0 to (d) where n = 3.
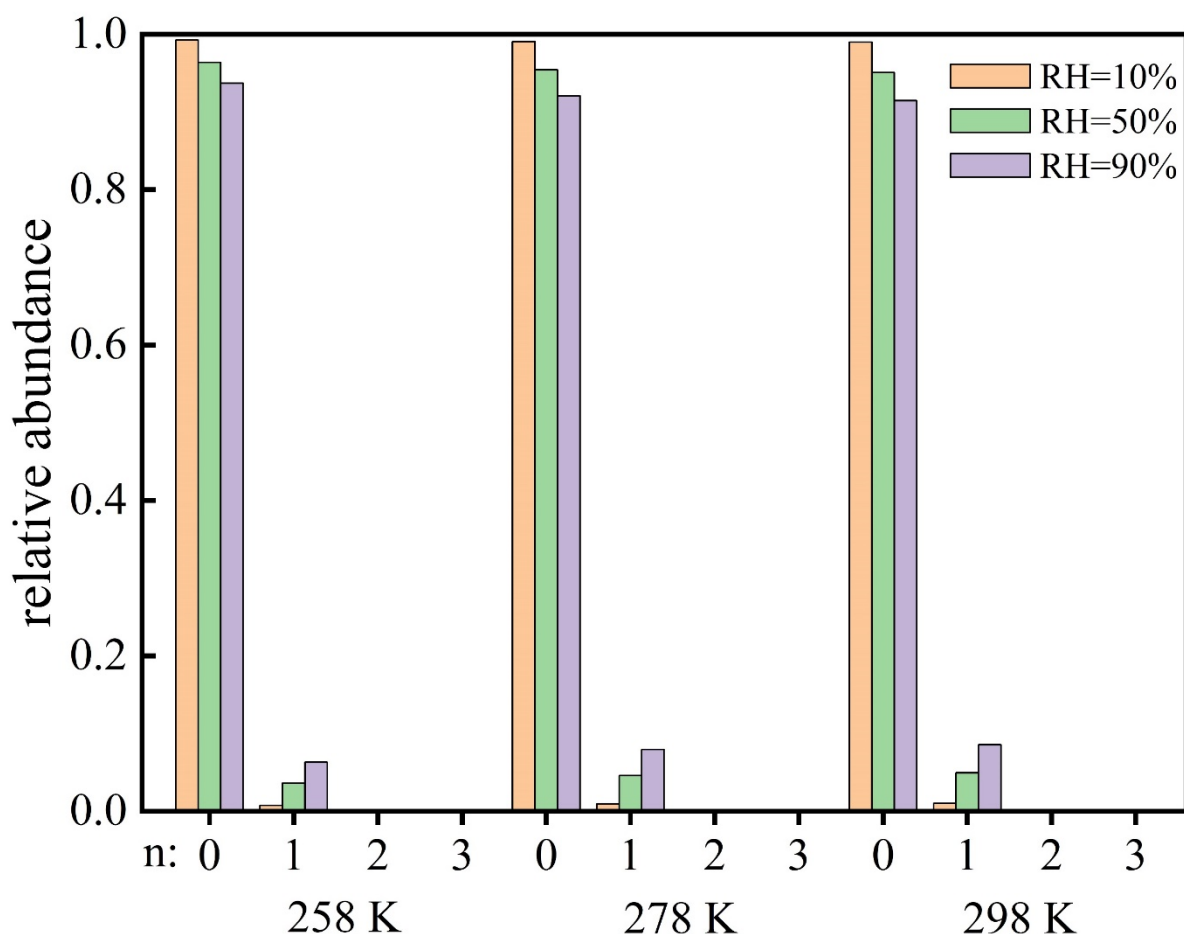
Figure S3. Equilibrium distribution of glycolic acid hydrates at different degrees of humidity (RH = 10%, 50% and 90%) and different temperatures (258 K, 278 K, and 298 K).

Related discussions

As shown in Table S2, the first water addition to GA at 298 K, with a Gibbs free energy change of -0.71 kcal mol^{-1}, are more favorable compared to the second and the third water additions, having free energy changes of 2.98 and 0.18 kcal mol^{-1}, respectively. Additionally, the energies decrease as the temperature decreases, and the energy of first water addition reaches to -1.96 kcal mol^{-1} at 258 K. Although the abundances of hydrated GA clusters, including mono-, di- and tri-hydrates, are slightly increased with increasing RH (relative humidity) (Figure S3 and Table S3), the hydration of GA is still weak at high RH. For example, the relative equilibrium abundance of GA hydrates is less than 7% at RH = 90% and 298 K. Therefore, the relative abundance of unhydrated GA is dominant at varying temperature and RH considered.

Figure S4. Identified lowest free energy structures of the $(GA)_x(SA)_y(DMA)_z$ ($0 \leq z \leq x + y \leq 3$) clusters at the DLPNO-CCSD(T)/aug-cc-pVTZ//M06-2X/6-311++G(3df,3pd) level of theory. The white, gray, red, and yellow balls represent hydrogen, carbon, oxygen, and sulfur atoms, respectively. Dashed black lines indicate hydrogen bonds.
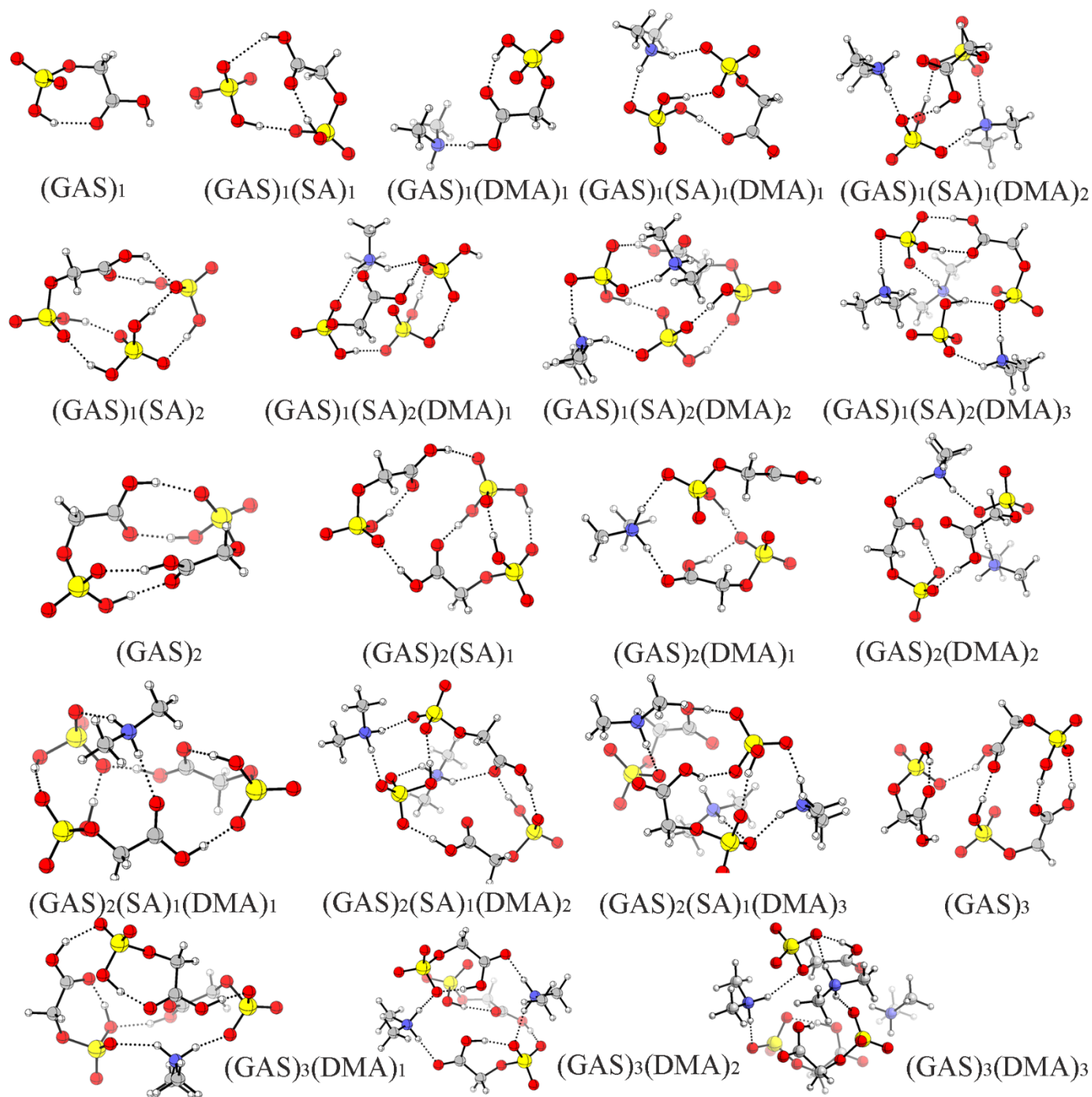
Figure S5. Identified lowest free energy structures of the $(GAS)_x(SA)_y(DMA)_z$ $(0 \leq z \leq x + y \leq 3)$ clusters at the DLPNO-CCSD(T)/aug-cc-pVTZ//M06-2X/6-311++G(3df,3pd) level of theory. The white, gray, red, and yellow balls represent hydrogen, carbon, oxygen, and sulfur atoms, respectively. Dashed black lines indicate hydrogen bonds.
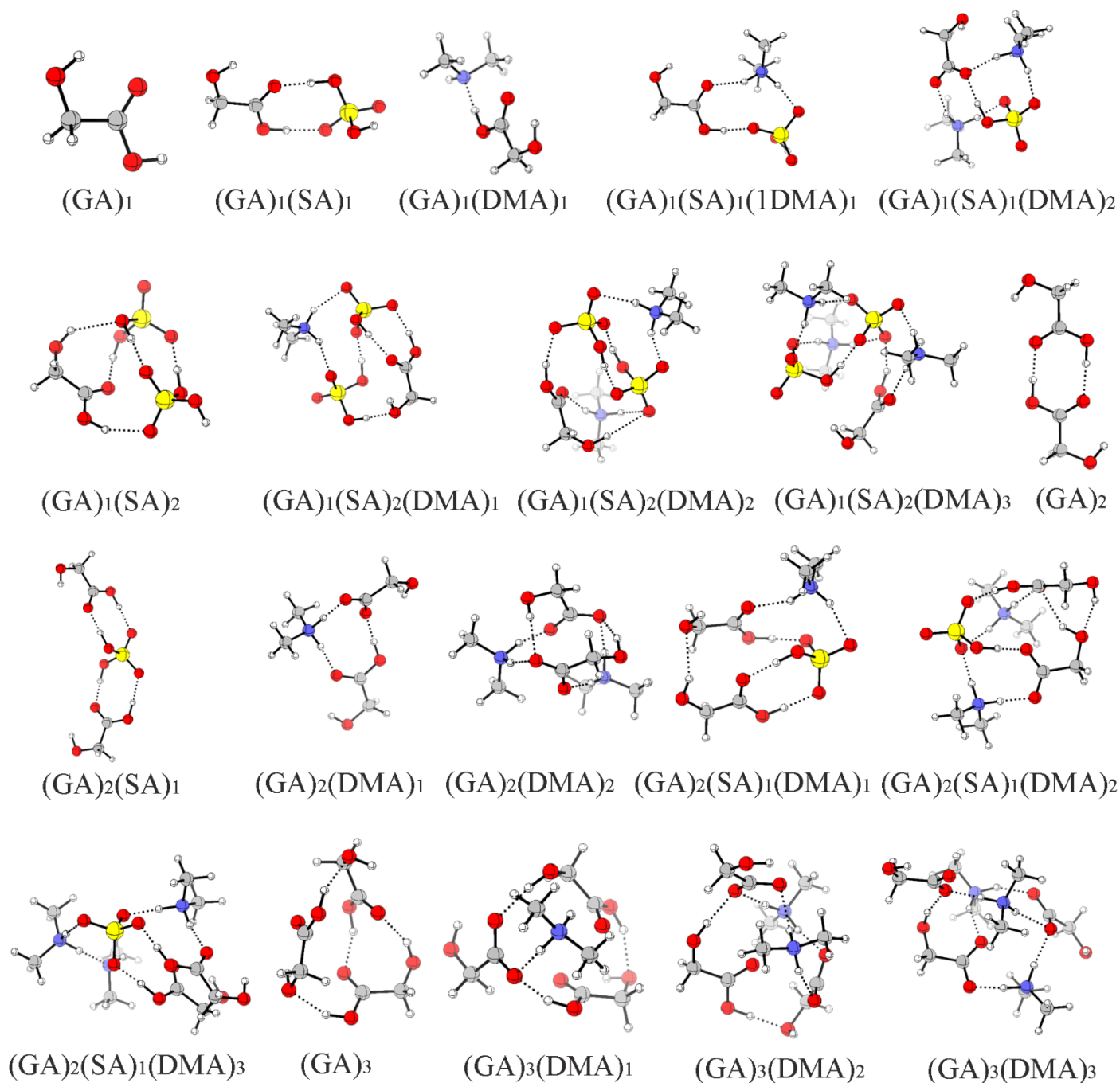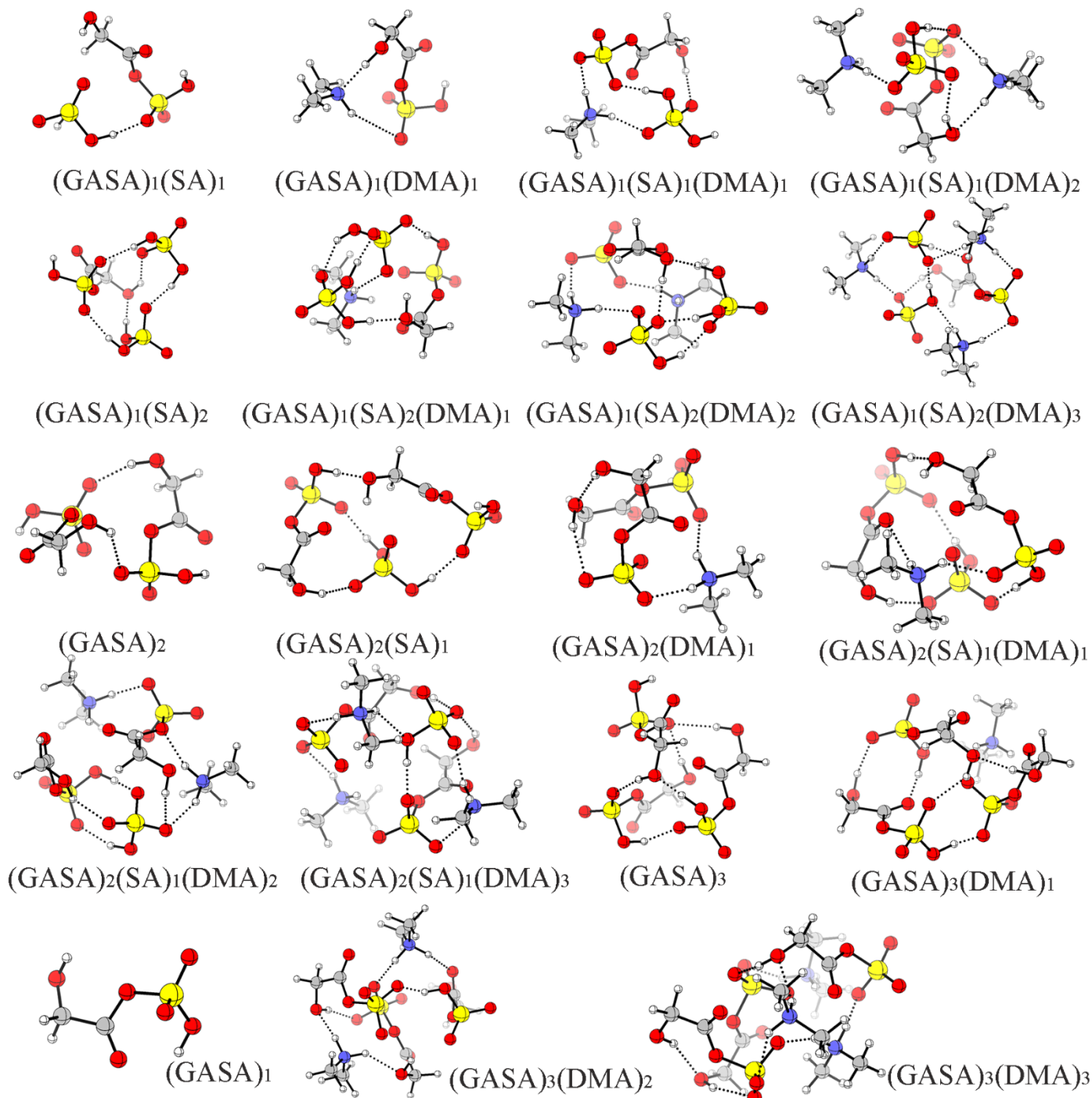
Figure S6. Identified lowest free energy structures of the (GASA)$_x$(SA)$_y$(DMA)$_z$ ($0 \leq z \leq x + y \leq 3$) clusters at the DLPNO-CCSD(T)/aug-cc-pVTZ//M06-2X/6-311++G(3df,3pd) level of theory. The white, gray, red, and yellow balls represent hydrogen, carbon, oxygen, and sulfur atoms, respectively. Dashed black lines indicate hydrogen bonds.
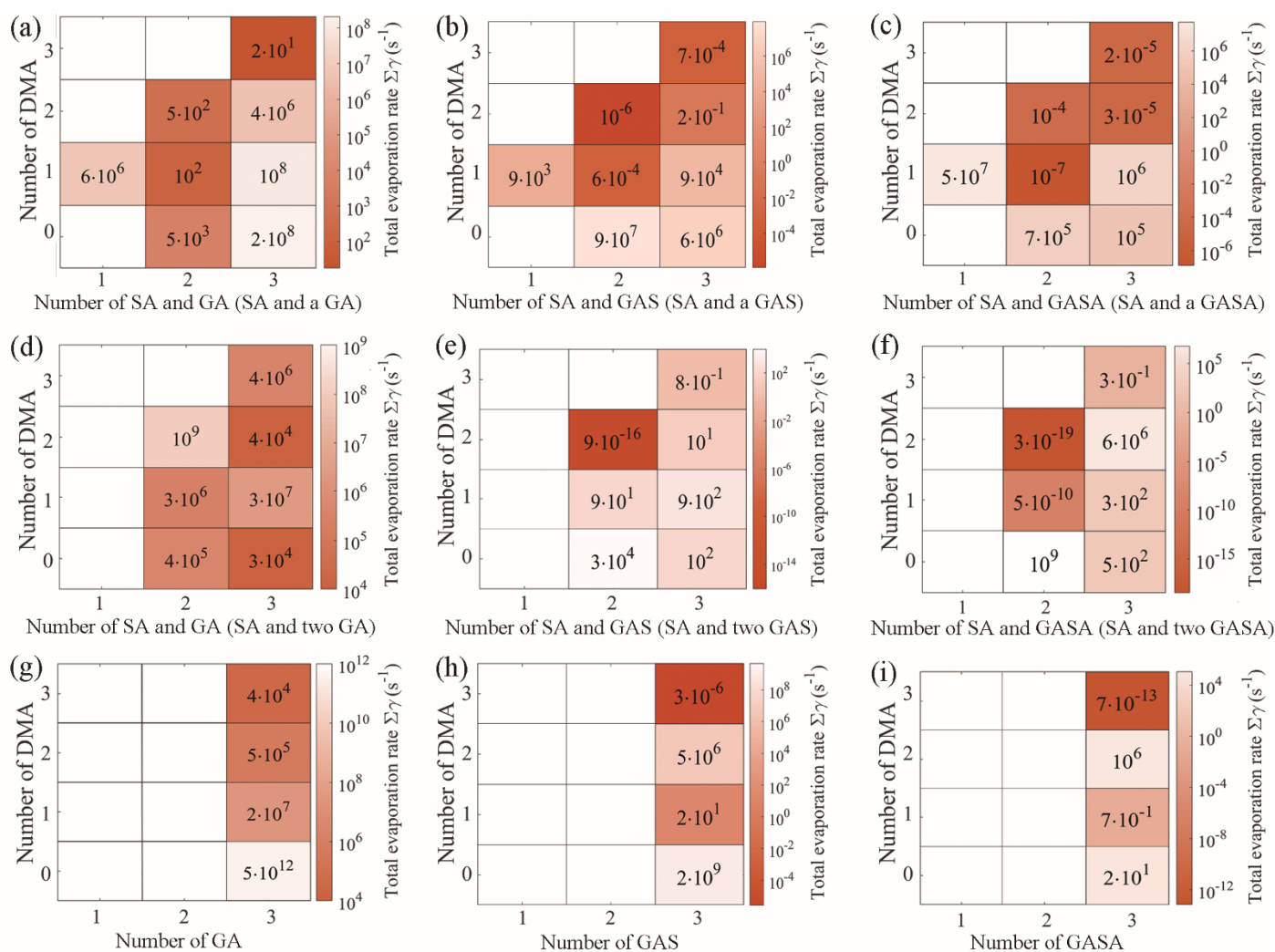
Figure S7. The evaporation rates of $(GA)_x(SA)_y(DMA)_z$ clusters $(1 \leq z \leq x + y \leq 3)$ (a, d, g; left panel), $(GAS)_x(SA)_y(DMA)_z$ clusters $(1 \leq z \leq x + y \leq 3)$ (b, e, h; center panel), and $(GASA)_x(SA)_y(DMA)_z$ clusters $(1 \leq z \leq x + y \leq 3)$ (c, f, i; right panel) at 278 K.

Related discussions

    The evaporation rates of the clusters in the GA-SA-DMA system, GAS-SA-DMA system and the GASA-SA-DMA system at 278 K are shown in Figure S5. As can be seen in Figure S5, the evaporation rates for the GA-SA-DMA clusters $((GA)_1(SA)_1(DMA)_2$, $(GA)_1(SA)_2(DMA)_3$, $(GA)_2(DMA)_2$, $(GA)_2(SA)_1(DMA)_3$, $(GA)_3(DMA)_3)$ along the diagonal line of the grid are much higher than those of corresponding GAS-SA-DMA and GASA-SA-DMA clusters, with a range from 10^1 to 10^9 s^{-1} in comparison to those of 10^{-1} to 10^{-19} s^{-1}. Furthermore, the evaporation of one DMA molecule or DMA involved small clusters (such as $(GA)_1(DMA)_1$, $(SA)_1(DMA)_1$, $(GAS)_1(DMA)_1$) was the main degradation pathway for clusters with the equal number of

acidic and base molecules, whereas the acidic monomer evaporation is dominant for clusters, in which the number of acidic molecules (GA, GAS, GASA and SA) is more than that of base molecules (DMA) (Table S3). Generally, clusters with low evaporation rates ($\leqslant 10^{-4}\,\text{s}^{-1}$) can be deemed as stable against evaporation, and most of the GAS-SA-DMA as well as GASA-SA-DMA clusters have lower evaporation rates than the corresponding GA-SA-DMA clusters, suggesting that the products (GAS/GASA)-involved clusters are more stable than the reactant (GA)-involved clusters. Therefore, we can conclude that GAS/GASA can form more stable clusters with SA-DMA than GA at the same size of acid and base molecules within all of the considered clusters.
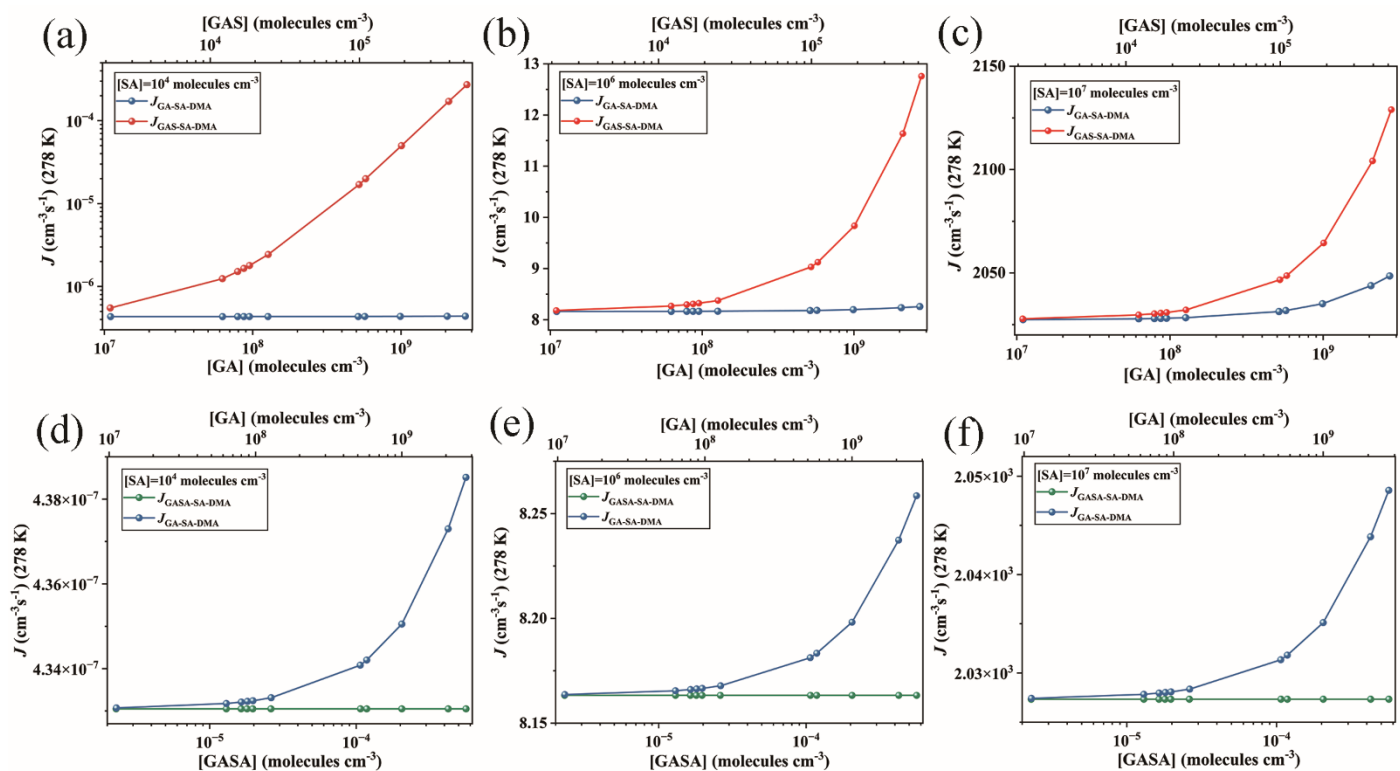
Figure S8. Simulated cluster formation rates J (cm^{-3}s^{-1}) as a function of monomer concentrations ([GA], [GAS], and [GASA], respectively) under different [SA] (a) (d) [SA] = 10^4, (b) (e) [SA] = 10^6, and (c) (f) [SA] = 10^7 molecules cm^{-3} at 278 K, [DMA] = 10^8 molecules cm^{-3}.
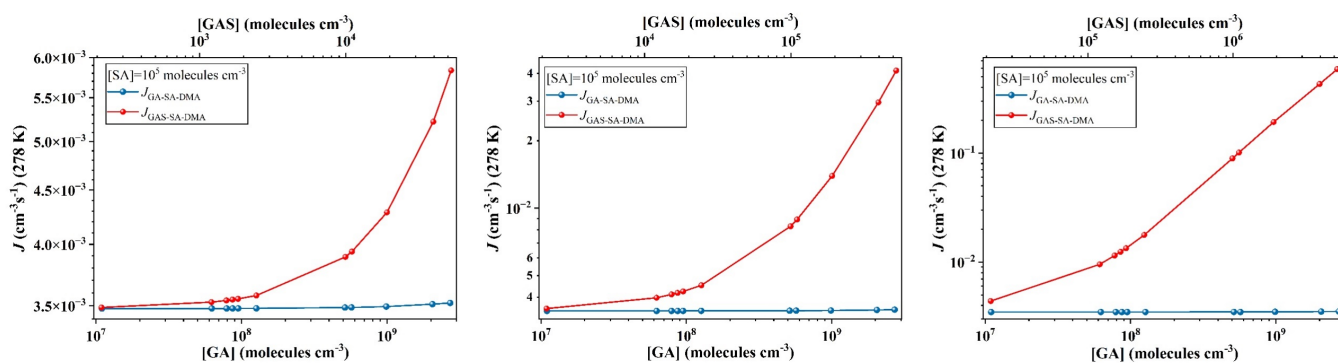
Figure S9. Simulated cluster formation rates J ($cm^{-3}s^{-1}$) as a function of monomer concentrations ([GA] and [GAS]) at 278 K and [SO_3] = 10^4 molecules cm^{-3} (left panel) [SO_3] = 10^5 molecules cm^{-3} (center panel) [SO_3] = 10^6 molecules cm^{-3} (right panel) under the condition of [DMA] = 10^8 molecules cm^{-3} and [SA] = 10^5 molecules cm^{-3}.

Related discussions

As the results displayed in Figure S9, we found that the cluster formation rate of GAS-SA-DMA system markedly increases with the increasing concentration of [GAS] compared to that of GA-SA-DMA system, especially in the case of [SO_3] = 10^6 molecules cm^{-3}, which $J_{GAS-SA-DMA}$ could be up to 2 orders of magnitude higher then $J_{GA-SA-DMA}$.

Figure S10. Main cluster growth pathway of (a) GAS-SA-DMA, and (b) (c) GA-SA-DMA nucleating system at 278 K, $[DMA] = 10^8$, $[SA] = 10^5$, $[GAS] = 10^5$ and $[GA] = 10^9$, 10^{10} molecules cm^{-3}, respectively. The black, green, and light orange arrows refer to the pathways of SA-DMA, GAS-SA-DMA and GA-SA-DMA, respectively.
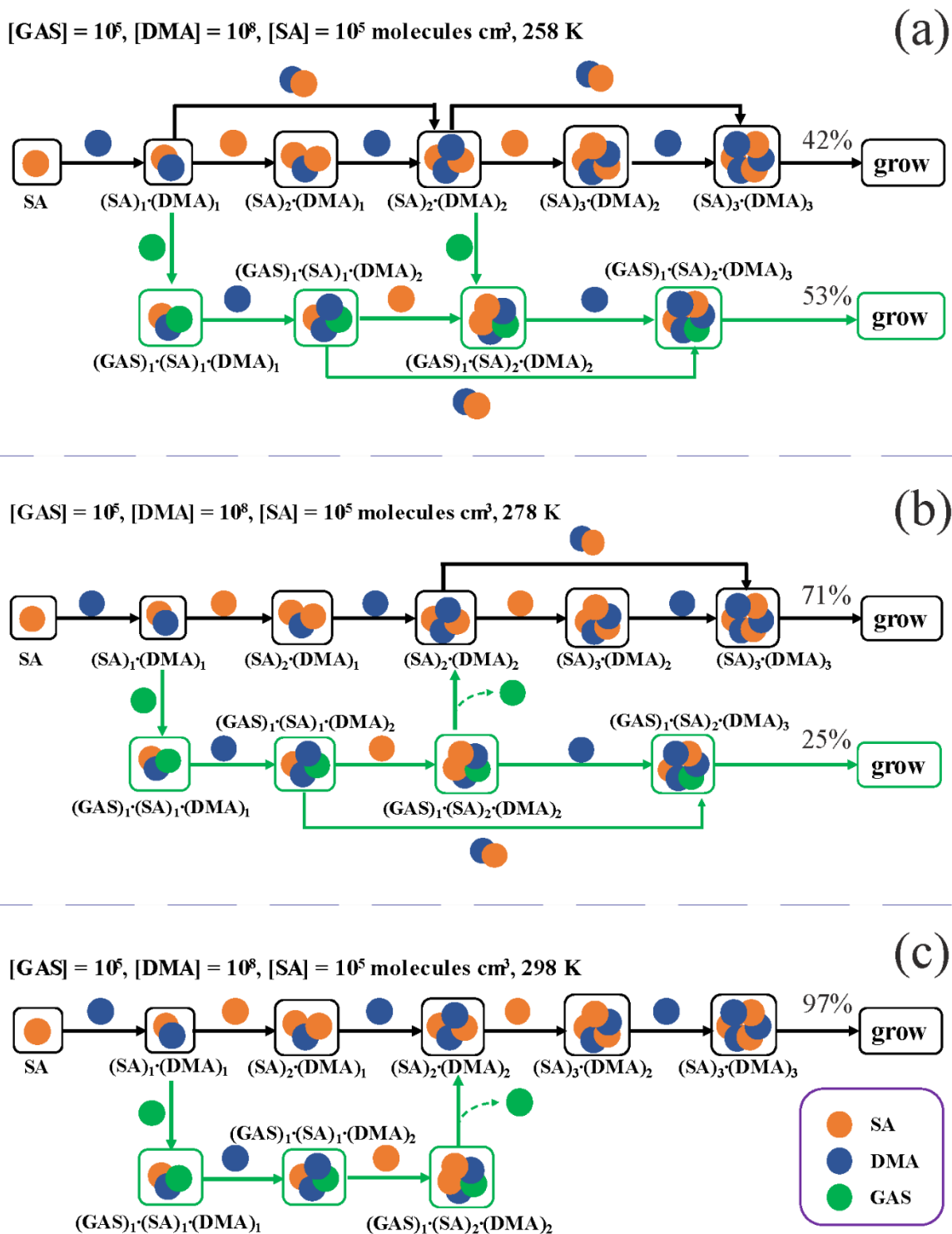
Figure S11. Main cluster growth pathway of GAS-SA-DMA nucleating system at $[GAS] = 10^5$, $[DMA] = 10^8$, $[SA] = 10^5$ molecules cm^{-3}, and (a) 258 K (b) 278 K (c) 298 K. The black and green arrows refer to the pathways of SA-DMA and GAS-SA-DMA, respectively. For clarity, other pathways that contributes less than 5% to the cluster growing out of the studied system are not shown.

Supporting information

Table S1 Equilibrium constants K_{eq} for pathway (1) (GA + SO$_3$)$_{-OH}$ → GAS and pathway (2) (GA + SO$_3$)$_{-COOH}$ → GASA and possible concentrations of GAS and GASA in the atmosphere, based on the formation Gibbs free energy (ΔG) at the DLPNO-CCSD(T)/aug-cc-pVTZ//M06-2X/6-311++G(3df,3pd) level of theory and 278 K, 101.3 KPa.

Reaction pathways	ΔG (kcal mol^{-1})	[GA] (molecules cm^{-3})	[SO$_3$] (molecules cm^{-3})	K_{eq} (cm^3 molecule^{-1})	[C] (molecules cm^{-3})
(GA + SO$_3$)$_{-OH}$ → GAS	-13.62	1.11×10^7- 2.72×10^9	10^5	1.93×10^{-9}	2.14×10^3- 5.24×10^5
(GA + SO$_3$)$_{-COOH}$ → GASA	-2.21	1.11×10^7- 2.72×10^9	10^5	2.07×10^{-18}	2.30×10^{-6}- 5.62×10^{-4}

Table S2 Thermodynamic data (in kcal mol^{-1}) of the stepwise hydration of glycolic acid (GA) calculated by the M06-2X/6-311++G(3df,3pd) method.

n	ΔG		
	258 K	278 K	298 K
	$(GA)(H_2O)_{n-1} + H_2O \leftrightarrow (GA)(H_2O)_n$		
1	-1.96	-1.33	-0.71
2	1.77	2.38	2.98
3	-1.07	-0.44	0.17

Table S3 Relative equilibrium abundance of GA hydrates at different degrees of humidity (RH = 10%, 20%, 40%, 50%, 90% and 100%) and different temperatures (258 K, 278 K, and 298 K)

258 K

RH	10%	20%	40%	50%	90%	100%
n=0	0.98970000	0.97970000	0.96020000	0.95070000	0.91460000	0.90600000
n=1	0.01026766	0.02032661	0.03984325	0.04931278	0.08539284	0.09398853
n=2	0.00000006	0.00000025	0.00000098	0.00000151	0.00000472	0.00000577
n=3	0.00000002	0.00000018	0.00000139	0.00000268	0.00001504	0.00002044

278 K

RH	10%	20%	40%	50%	90%	100%
n=0	0.99050000	0.98120000	0.96310000	0.95430000	0.92070000	0.91260000
n=1	0.00948502	0.01879180	0.03689036	0.04569154	0.07934438	0.08738994
n=2	0.00000001	0.00000004	0.00000015	0.00000023	0.00000073	0.00000089
n=3	0.00000000	0.00000001	0.00000009	0.00000017	0.00000095	0.00000130

298 K

RH	10%	20%	40%	50%	90%	100%
n=0	0.99260000	0.98530000	0.97100000	0.96400000	0.93700000	0.93050000
n=1	0.00741927	0.01472926	0.02903091	0.03602716	0.06303219	0.06954867
n=2	0.00000000	0.00000000	0.00000001	0.00000002	0.00000006	0.00000008
n=3	0.00000000	0.00000000	0.00000000	0.00000000	0.00000002	0.00000003

Table S4. Calculated Gibbs free energy changes (ΔG) of the formation of heterotrimers consisting of H_2SO_4, base (ammonia/DMA), and GA/GAS/GASA at the temperature of 278 K and pressure of 101.3 KPa.

clusters	ΔG (kcal mol^{-1}) GA-SA-ammonia [a]	ΔG (kcal mol^{-1}) GA-SA-DMA	ΔG (kcal mol^{-1}) GAS-SA-DMA	ΔG (kcal mol^{-1}) GASA-SA-DMA
Org-base	-2.74	-4.23	-7.83	-3.06
Org-SA	-7.55	-7.97	-2.58	-5.27
Org-SA-base	-14.90	-23.12	-29.90	-34.54
Org-SA-2base	-16.68	-32.66	-50.48	-52.57
Org-2SA	-14.55	-11.70	-13.58	-15.75
Org-2SA-base	-28.21	-37.71	-41.62	-40.26
Org-2SA-2base	-36.81	-55.95	-65.39	-71.31
Org-2SA-3base	-41.21	-67.68	-82.56	-90.30
2Org	-5.37	-5.17	-6.68	-0.77
2Org-base	-4.33	-10.05	-18.20	-27.65
2Org-2base	-2.35	-11.59	-50.36	-64.19
2Org-SA	-14.87	-15.04	-16.86	-14.54
2Org-SA-base	-19.96	-26.48	-38.94	-44.23
2Org-SA-2base	-20.99	-39.72	-62.20	-68.50
2Org-SA-3base	-23.42	-44.48	-76.48	-90.80
3Org	-5.24	-1.81	-7.71	-11.82
3Org-base	-6.87	-13.61	-29.49	-40.64
3Org-2base	-6.98	-20.11	-54.73	-69.36
3Org-3base	-3.20	-27.43	-78.18	-98.00

a The data is from J. Chem. Phys. 146, 184308 (2017) "The enhancement mechanism of glycolic acid on the formation of atmospheric sulfuric acid–ammonia molecular clusters" calculated at the level of M06-2X/6-311++G(3df,3pd)//CCSD(T)-F12/VDZ-F12 (Zhang et al., 2017).

Table S5. Calculated Gibbs free energy changes (ΔG) of the formation of heterotrimers consisting of H2SO4, base (ammonia/DMA), and GA/GAS/GASA at the temperature of 298 K and pressure of 101.3 KPa.

clusters	ΔG (kcal mol^{-1}) SA-GA-ammonia [a]	ΔG (kcal mol^{-1}) SA-GA-DMA	ΔG (kcal mol^{-1}) SA-GAS-DMA	ΔG (kcal mol^{-1}) SA-GASA-DMA
Org-base	-2.11	-3.50	-7.10	-2.37
Org-SA	-6.83	-7.28	-1.78	-4.51
Org-SA-base	-13.51	-21.76	-28.35	-32.90
Org-SA-2base	-14.55	-30.36	-48.13	-50.06
Org-2SA	-12.94	-10.10	-11.86	-14.04
Org-2SA-base	-25.95	-35.22	-39.15	-37.64
Org-2SA-2base	-33.76	-52.74	-62.14	-67.93
Org-2SA-3base	-37.48	-63.71	-78.55	-86.19
2Org	-4.62	-4.40	-5.76	0.13
2Org-base	-2.97	-8.64	-16.54	-25.84
2Org-2base	-0.32	-9.03	-47.82	-61.62
2Org-SA	-13.39	-13.60	-15.13	-12.75
2Org-SA-base	-17.74	-24.08	-36.49	-41.54
2Org-SA-2base	-17.78	-36.51	-58.92	-65.15
2Org-SA-3base	-19.65	-40.59	-72.36	-86.50
3Org	-3.76	-0.12	-5.99	-10.01
3Org-base	-4.67	-11.16	-26.82	-37.95
3Org-2base	-3.94	-16.80	-51.34	-65.78
3Org-3base	-17.78	-23.60	-74.01	-93.69

a The data is from J. Chem. Phys. 146, 184308 (2017) "The enhancement mechanism of glycolic acid on the formation of atmospheric sulfuric acid–ammonia molecular clusters" calculated at the level of M06-2X/6-311++G(3df,3pd)//CCSD(T)-F12/VDZ-F12 (Zhang et al., 2017).

Supporting information

Table S6. Evaporation rate coefficients (s^{-1}) for simulated evaporation pathways of GA-involved, GAS-involved and GASA-involved clusters at 278 K and 101.3 KPa obtained by the ACDC simulations.

Evaporation pathways	Evaporation rate coefficients
$(SA)_2 \rightarrow SA + SA$	1.40×10^2
$(SA)_3 \rightarrow (SA)_2 + SA$	1.01×10^5
$(SA)_1(DMA)_1 \rightarrow DMA + SA$	7.46×10^{-1}
$(SA)_2(DMA)_1 \rightarrow (SA)_1(DMA)_1 + SA$	3.92×10^{-8}
$(SA)_2(DMA)_1 \rightarrow DMA + (SA)_2$	9.95×10^{-11}
$(SA)_3(DMA)_1 \rightarrow (SA)_2(DMA)_1 + SA$	7.15×10^{-1}
$(SA)_3(DMA)_1 \rightarrow (SA)_1(DMA)_1 + (SA)_2$	8.07×10^{-11}
$(SA)_3(DMA)_1 \rightarrow DMA + (SA)_3$	6.80×10^{-16}
$(SA)_2(DMA)_2 \rightarrow (SA)_2(DMA)_1 + DMA$	2.32×10^{-3}
$(SA)_2(DMA)_2 \rightarrow (SA)_1(DMA)_1 + (SA)_1(DMA)_1$	5.15×10^{-11}
$(SA)_3(DMA)_2 \rightarrow (SA)_2(DMA)_2 + SA$	2.11×10^{-4}
$(SA)_3(DMA)_2 \rightarrow (SA)_3(DMA)_1 + DMA$	6.66×10^{-7}
$(SA)_3(DMA)_2 \rightarrow (SA)_2(DMA)_1 + (SA)_1(DMA)_1$	4.78×10^{-7}
$(SA)_3(DMA)_3 \rightarrow (SA)_3(DMA)_2 + DMA$	6.58×10^{-4}
$(SA)_3(DMA)_3 \rightarrow (SA)_2(DMA)_2 + (SA)_1(DMA)_1$	1.24×10^{-7}
$(SA)_1(GA)_1 \rightarrow GA + SA$	5.09×10^3
$(SA)_2(GA)_1 \rightarrow (SA)_1(GA)_1 + SA$	1.19×10^7
$(SA)_2(GA)_1 \rightarrow GA + (SA)_2$	1.94×10^8
$(GA)_2 \rightarrow GA + GA$	4.11×10^5
$(SA)_1(GA)_2 \rightarrow (GA)_2 + SA$	1.91×10^2
$(SA)_1(GA)_2 \rightarrow (SA)_1(GA)_1 + GA$	2.81×10^4
$(GA)_3 \rightarrow (GA)_2 + GA$	4.58×10^{12}
$(GA)_1(DMA)_1 \rightarrow GA + DMA$	6.23×10^6
$(SA)_1(GA)_1(DMA)_1 \rightarrow (GA)_1(DMA)_1 + SA$	1.55×10^{-5}
$(SA)_1(GA)_1(DMA)_1 \rightarrow (SA)_1(GA)_1 + DMA$	1.83×10^{-2}

$(SA)_1(GA)_1(DMA)_1 \rightarrow GA + (SA)_1(DMA)_1$ $\qquad 1.17 \times 10^2$

$(SA)_2(GA)_1(DMA)_1 \rightarrow (SA)_1(GA)_1(DMA)_1 + SA$ $\qquad 3.98 \times 10^{-2}$

$(SA)_2(GA)_1(DMA)_1 \rightarrow (GA)_1(DMA)_1 + (SA)_2$ $\qquad 1.65 \times 10^{-9}$

$(SA)_2(GA)_1(DMA)_1 \rightarrow (SA)_2(GA)_1 + DMA$ $\qquad 5.91 \times 10^{-11}$

$(SA)_2(GA)_1(DMA)_1 \rightarrow (SA)_1(GA)_1 + (SA)_1(DMA)_1$ $\qquad 7.66 \times 10^{-4}$

$(SA)_2(GA)_1(DMA)_1 \rightarrow GA + (SA)_2(DMA)_1$ $\qquad 1.10 \times 10^8$

$(GA)_2(DMA)_1 \rightarrow (GA)_2 + DMA$ $\qquad 2.32 \times 10^6$

$(GA)_2(DMA)_1 \rightarrow (GA)_1(DMA)_1 + GA$ $\qquad 2.90 \times 10^5$

$(SA)_1(GA)_2(DMA)_1 \rightarrow (GA)_2(DMA)_1 + SA$ $\qquad 1.48 \times 10^{-3}$

$(SA)_1(GA)_2(DMA)_1 \rightarrow (SA)_1(GA)_2 + DMA$ $\qquad 1.75 \times 10^1$

$(SA)_1(GA)_2(DMA)_1 \rightarrow (GA)_2 + (SA)_1(DMA)_1$ $\qquad 3.38 \times 10^3$

$(SA)_1(GA)_2(DMA)_1 \rightarrow (SA)_1(GA)_1(DMA)_1 + GA$ $\qquad 2.59 \times 10^7$

$(SA)_1(GA)_2(DMA)_1 \rightarrow (GA)_1(DMA)_1 + (SA)_1(GA)_1$ $\qquad 6.62 \times 10^{-2}$

$(GA)_3(DMA)_1 \rightarrow (GA)_3 + DMA$ $\qquad 9.61 \times 10^0$

$(GA)_3(DMA)_1 \rightarrow (GA)_2(DMA)_1 + GA$ $\qquad 1.83 \times 10^7$

$(GA)_3(DMA)_1 \rightarrow (GA)_1(DMA)_1 + (GA)_2$ $\qquad 5.59 \times 10^6$

$(SA)_1(GA)_1(DMA)_2 \rightarrow (SA)_1(GA)_1(DMA)_1 + DMA$ $\qquad 5.40 \times 10^2$

$(SA)_1(GA)_1(DMA)_2 \rightarrow (GA)_1(DMA)_1 + (SA)_1(DMA)_1$ $\qquad 8.83 \times 10^{-3}$

$(SA)_2(GA)_1(DMA)_2 \rightarrow (SA)_1(GA)_1(DMA)_2 + SA$ $\qquad 6.42 \times 10^{-9}$

$(SA)_2(GA)_1(DMA)_2 \rightarrow (SA)_2(GA)_1(DMA)_1 + (DMA)_1$ $\qquad 8.50 \times 10^{-5}$

$(SA)_2(GA)_1(DMA)_2 \rightarrow (SA)_1(GA)_1(DMA)_1 + (SA)_1(DMA)_1$ $\qquad 3.21 \times 10^{-6}$

$(SA)_2(GA)_1(DMA)_2 \rightarrow (GA)_1(DMA)_1 + (SA)_2(DMA)_1$ $\qquad 1.18 \times 10^{-3}$

$(SA)_2(GA)_1(DMA)_2 \rightarrow GA + (SA)_2(DMA)_2$ $\qquad 3.90 \times 10^6$

$(GA)_2(DMA)_2 \rightarrow (GA)_2(DMA)_1 + DMA$ $\qquad 1.11 \times 10^9$

$(GA)_2(DMA)_2 \rightarrow (GA)_1(DMA)_1 + (GA)_1(DMA)_1$ $\qquad 2.11 \times 10^7$

$(SA)_1(GA)_2(DMA)_2 \rightarrow (GA)_2(DMA)_2 + SA$ $\qquad 1.04 \times 10^{-12}$

$(SA)_1(GA)_2(DMA)_2 \rightarrow (SA)_1(GA)_2(DMA)_1 + DMA$ $\qquad 7.60 \times 10^{-1}$

$(SA)_1(GA)_2(DMA)_2 \rightarrow (GA)_2(DMA)_1 + (SA)_1(DMA)_1$ $\qquad 1.01 \times 10^{-3}$

$(SA)_1(GA)_2(DMA)_2 \rightarrow (SA)_1(GA)_1(DMA)_2 + GA$ $\qquad 3.53 \times 10^4$

$(SA)_1(GA)_2(DMA)_2 \rightarrow (SA)_1(GA)_1(DMA)_1 + (GA)_1(DMA)_1$ 2.35×10^0

$(GA)_3(DMA)_2 \rightarrow (GA)_3(DMA)_1 + DMA$ 1.58×10^5

$(GA)_3(DMA)_2 \rightarrow (GA)_2(DMA)_2 + GA$ 2.54×10^3

$(GA)_3(DMA)_2 \rightarrow (GA)_2(DMA)_1 + (GA)_1(DMA)_1$ 3.30×10^5

$(SA)_2(GA)_1(DMA)_3 \rightarrow (SA)_2(GA)_1(DMA)_2 + DMA$ 1.23×10^1

$(SA)_2(GA)_1(DMA)_3 \rightarrow (SA)_1(GA)_1(DMA)_2 + (SA)_1(DMA)_1$ 6.72×10^{-8}

$(SA)_2(GA)_1(DMA)_3 \rightarrow (GA)_1(DMA)_1 + (SA)_2(DMA)_2$ 5.45×10^0

$(SA)_1(GA)_2(DMA)_3 \rightarrow (SA)_1(GA)_2(DMA)_2 + DMA$ 3.78×10^6

$(SA)_1(GA)_2(DMA)_3 \rightarrow (GA)_2(DMA)_2 + (SA)_1(DMA)_1$ 3.19×10^{-6}

$(SA)_1(GA)_2(DMA)_3 \rightarrow (SA)_1(GA)_1(DMA)_2 + (GA)_1(DMA)_1$ 1.45×10^4

$(GA)_3(DMA)_3 \rightarrow (GA)_3(DMA)_2 + DMA$ 3.75×10^4

$(GA)_3(DMA)_3 \rightarrow (GA)_2(DMA)_2 + (GA)_1(DMA)_1$ 9.97×10^0

$(SA)_1(GAS)_1 \rightarrow GAS + SA$ 8.70×10^7

$(SA)_2(GAS)_1 \rightarrow (SA)_1(GAS)_1 + SA$ 2.34×10^1

$(SA)_2(GAS)_1 \rightarrow GAS + (SA)_2$ 6.50×10^6

$(GAS)_2 \rightarrow GAS + GAS$ 2.65×10^4

$(SA)_1(GAS)_2 \rightarrow (GAS)_2 + SA$ 1.08×10^2

$(SA)_1(GAS)_2 \rightarrow (SA)_1(GAS)_1 + GAS$ 5.99×10^{-2}

$(GAS)_3 \rightarrow (GAS)_2 + GAS$ 1.64×10^9

$(GAS)_1(DMA)_1 \rightarrow GAS + DMA$ 9.21×10^3

$(SA)_1(GAS)_1(DMA)_1 \rightarrow (GAS)_1(DMA)_1 + SA$ 4.96×10^{-8}

$(SA)_1(GAS)_1(DMA)_1 \rightarrow (SA)_1(GAS)_1 + DMA$ 5.04×10^{-12}

$(SA)_1(GAS)_1(DMA)_1 \rightarrow GAS + (SA)_1(DMA)_1$ 5.51×10^{-4}

$(SA)_2(GAS)_1(DMA)_1 \rightarrow (SA)_1(GAS)_1(DMA)_1 + SA$ 7.18×10^0

$(SA)_2(GAS)_1(DMA)_1 \rightarrow (GAS)_1(DMA)_1 + (SA)_2$ 9.51×10^{-10}

$(SA)_2(GAS)_1(DMA)_1 \rightarrow (SA)_2(GAS)_1 + DMA$ 1.50×10^{-12}

$(SA)_2(GAS)_1(DMA)_1 \rightarrow (SA)_1(GAS)_1 + (SA)_1(DMA)_1$ 3.81×10^{-11}

$(SA)_2(GAS)_1(DMA)_1 \rightarrow GAS + (SA)_2(DMA)_1$ 9.37×10^4

$(GAS)_2(DMA)_1 \rightarrow (GAS)_2 + DMA$ 1.42×10^1

$(GAS)_2(DMA)_1 \rightarrow (GAS)_1(DMA)_1 + GAS$	7.72×10^1
$(SA)_1(GAS)_2(DMA)_1 \rightarrow (GAS)_2(DMA)_1 + SA$	6.08×10^{-7}
$(SA)_1(GAS)_2(DMA)_1 \rightarrow (SA)_1(GAS)_2 + DMA$	7.76×10^{-8}
$(SA)_1(GAS)_2(DMA)_1 \rightarrow (GAS)_2 + (SA)_1(DMA)_1$	8.48×10^{-6}
$(SA)_1(GAS)_2(DMA)_1 \rightarrow (SA)_1(GAS)_1(DMA)_1 + GAS$	8.86×10^2
$(SA)_1(GAS)_2(DMA)_1 \rightarrow (GAS)_1(DMA)_1 + (SA)_1(GAS)_1$	4.24×10^{-13}
$(GAS)_3(DMA)_1 \rightarrow (GAS)_3 + DMA$	1.39×10^{-7}
$(GAS)_3(DMA)_1 \rightarrow (GAS)_2(DMA)_1 + GAS$	1.55×10^1
$(GAS)_3(DMA)_1 \rightarrow (GAS)_1(DMA)_1 + (GAS)_2$	1.95×10^{-2}
$(SA)_1(GAS)_1(DMA)_2 \rightarrow (SA)_1(GAS)_1(DMA)_1 + DMA$	1.13×10^{-6}
$(SA)_1(GAS)_1(DMA)_2 \rightarrow (GAS)_1(DMA)_1 + (SA)_1(DMA)_1$	5.90×10^{-14}
$(SA)_2(GAS)_1(DMA)_2 \rightarrow (SA)_1(GAS)_1(DMA)_2 + SA$	2.47×10^{-2}
$(SA)_2(GAS)_1(DMA)_2 \rightarrow (SA)_2(GAS)_1(DMA)_1 + DMA$	3.80×10^{-9}
$(SA)_2(GAS)_1(DMA)_2 \rightarrow (SA)_1(GAS)_1(DMA)_1 + (SA)_1(DMA)_1$	2.58×10^{-8}
$(SA)_2(GAS)_1(DMA)_2 \rightarrow (GAS)_1(DMA)_1 + (SA)_2(DMA)_1$	3.04×10^{-8}
$(SA)_2(GAS)_1(DMA)_2 \rightarrow GAS + (SA)_2(DMA)_2$	1.48×10^{-1}
$(GAS)_2(DMA)_2 \rightarrow (GAS)_2(DMA)_1 + DMA$	9.33×10^{-16}
$(GAS)_2(DMA)_2 \rightarrow (GAS)_1(DMA)_1 + (GAS)_1(DMA)_1$	3.20×10^{-18}
$(SA)_1(GAS)_2(DMA)_2 \rightarrow (GAS)_2(DMA)_2 + SA$	6.61×10^0
$(SA)_1(GAS)_2(DMA)_2 \rightarrow (SA)_1(GAS)_2(DMA)_1 + DMA$	9.94×10^{-9}
$(SA)_1(GAS)_2(DMA)_2 \rightarrow (GAS)_2(DMA)_1 + (SA)_1(DMA)_1$	5.42×10^{-15}
$(SA)_1(GAS)_2(DMA)_2 \rightarrow (SA)_1(GAS)_1(DMA)_2 + GAS$	7.56×10^0
$(SA)_1(GAS)_2(DMA)_2 \rightarrow (SA)_1(GAS)_1(DMA)_1 + (GAS)_1(DMA)_1$	7.13×10^{-10}
$(GAS)_3(DMA)_2 \rightarrow (GAS)_3(DMA)_1 + DMA$	2.85×10^{-10}
$(GAS)_3(DMA)_2 \rightarrow (GAS)_2(DMA)_2 + GAS$	4.62×10^6
$(GAS)_3(DMA)_2 \rightarrow (GAS)_2(DMA)_1 + (GAS)_1(DMA)_1$	3.24×10^{-13}
$(SA)_2(GAS)_1(DMA)_3 \rightarrow (SA)_2(GAS)_1(DMA)_2 + DMA$	6.38×10^{-4}
$(SA)_2(GAS)_1(DMA)_3 \rightarrow (SA)_1(GAS)_1(DMA)_2 + (SA)_1(DMA)_1$	1.34×10^{-5}
$(SA)_2(GAS)_1(DMA)_3 \rightarrow (GAS)_1(DMA)_1 + (SA)_2(DMA)_2$	7.27×10^{-9}

$(SA)_1(GAS)_2(DMA)_3 \rightarrow (SA)_1(GAS)_2(DMA)_2 + DMA$	1.23×10^{-1}
$(SA)_1(GAS)_2(DMA)_3 \rightarrow (GAS)_2(DMA)_2 + (SA)_1(DMA)_1$	6.65×10^{-1}
$(SA)_1(GAS)_2(DMA)_3 \rightarrow (SA)_1(GAS)_1(DMA)_2 + (GAS)_1(DMA)_1$	6.86×10^{-5}
$(GAS)_3(DMA)_3 \rightarrow (GAS)_3(DMA)_2 + DMA$	7.91×10^{-9}
$(GAS)_3(DMA)_3 \rightarrow (GAS)_2(DMA)_2 + (GAS)_1(DMA)_1$	2.58×10^{-6}
$(SA)_1(GASA)_1 \rightarrow GASA + SA$	6.74×10^{5}
$(SA)_2(GASA)_1 \rightarrow (SA)_1(GASA)_1 + SA$	5.89×10^{1}
$(SA)_2(GASA)_1 \rightarrow GASA + (SA)_2$	1.27×10^{5}
$(GASA)_2 \rightarrow GASA + GASA$	1.19×10^{9}
$(SA)_1(GASA)_2 \rightarrow (GASA)_2 + SA$	1.62×10^{-1}
$(SA)_1(GASA)_2 \rightarrow (SA)_1(GASA)_1 + GASA$	5.20×10^{2}
$(GASA)_3 \rightarrow (GASA)_2 + GASA$	2.17×10^{1}
$(GASA)_1(DMA)_1 \rightarrow GASA + DMA$	5.14×10^{7}
$(SA)_1(GASA)_1(DMA)_1 \rightarrow (GASA)_1(DMA)_1 + SA$	1.99×10^{-15}
$(SA)_1(GASA)_1(DMA)_1 \rightarrow (SA)_1(GASA)_1 + DMA$	1.46×10^{-13}
$(SA)_1(GASA)_1(DMA)_1 \rightarrow GASA + (SA)_1(DMA)_1$	1.23×10^{-7}
$(SA)_2(GASA)_1(DMA)_1 \rightarrow (SA)_1(GASA)_1(DMA)_1 + SA$	3.77×10^{5}
$(SA)_2(GASA)_1(DMA)_1 \rightarrow (GASA)_1(DMA)_1 + (SA)_2$	2.00×10^{-12}
$(SA)_2(GASA)_1(DMA)_1 \rightarrow (SA)_2(GASA)_1 + DMA$	9.05×10^{-10}
$(SA)_2(GASA)_1(DMA)_1 \rightarrow (SA)_1(GASA)_1 + (SA)_1(DMA)_1$	5.78×10^{-8}
$(SA)_2(GASA)_1(DMA)_1 \rightarrow GASA + (SA)_2(DMA)_1$	1.10×10^{6}
$(GASA)_2(DMA)_1 \rightarrow (GASA)_2 + DMA$	1.16×10^{-11}
$(GASA)_2(DMA)_1 \rightarrow (GASA)_1(DMA)_1 + GASA$	5.09×10^{-10}
$(SA)_1(GASA)_2(DMA)_1 \rightarrow (GASA)_2(DMA)_1 + SA$	1.13×10^{-3}
$(SA)_1(GASA)_2(DMA)_1 \rightarrow (SA)_1(GASA)_2 + DMA$	7.91×10^{-14}
$(SA)_1(GASA)_2(DMA)_1 \rightarrow (GASA)_2 + (SA)_1(DMA)_1$	1.30×10^{-14}
$(SA)_1(GASA)_2(DMA)_1 \rightarrow (SA)_1(GASA)_1(DMA)_1 + GASA$	2.71×10^{2}
$(SA)_1(GASA)_2(DMA)_1 \rightarrow (GASA)_1(DMA)_1 + (SA)_1(GASA)_1$	6.7×10^{-19}
$(GASA)_3(DMA)_1 \rightarrow (GASA)_3 + DMA$	4.00×10^{-13}

$(GASA)_3(DMA)_1 \rightarrow (GASA)_2(DMA)_1 + GASA$	7.19×10^{-1}
$(GASA)_3(DMA)_1 \rightarrow (GASA)_1(DMA)_1 + (GASA)_2$	1.33×10^{-19}
$(SA)_1(GASA)_1(DMA)_2 \rightarrow (SA)_1(GASA)_1(DMA)_1 + DMA$	1.14×10^{-4}
$(SA)_1(GASA)_1(DMA)_2 \rightarrow (GASA)_1(DMA)_1 + (SA)_1(DMA)_1$	2.38×10^{-19}
$(SA)_2(GASA)_1(DMA)_2 \rightarrow (SA)_1(GASA)_1(DMA)_2 + SA$	2.44×10^{-5}
$(SA)_2(GASA)_1(DMA)_2 \rightarrow (SA)_2(GASA)_1(DMA)_1 + DMA$	7.19×10^{-15}
$(SA)_2(GASA)_1(DMA)_2 \rightarrow (SA)_1(GASA)_1(DMA)_1 + (SA)_1(DMA)_1$	2.57×10^{-9}
$(SA)_2(GASA)_1(DMA)_2 \rightarrow (GASA)_1(DMA)_1 + (SA)_2(DMA)_1$	1.21×10^{-16}
$(SA)_2(GASA)_1(DMA)_2 \rightarrow GASA + (SA)_2(DMA)_2$	3.30×10^{-6}
$(GASA)_2(DMA)_2 \rightarrow (GASA)_2(DMA)_1 + DMA$	3.38×10^{-19}
$(GASA)_2(DMA)_2 \rightarrow (GASA)_1(DMA)_1 + (GASA)_1(DMA)_1$	1.37×10^{-36}
$(SA)_1(GASA)_2(DMA)_2 \rightarrow (GASA)_2(DMA)_2 + SA$	5.51×10^{6}
$(SA)_1(GASA)_2(DMA)_2 \rightarrow (SA)_1(GASA)_2(DMA)_1 + DMA$	1.62×10^{-9}
$(SA)_1(GASA)_2(DMA)_2 \rightarrow (GASA)_2(DMA)_1 + (SA)_1(DMA)_1$	1.64×10^{-12}
$(SA)_1(GASA)_2(DMA)_2 \rightarrow (SA)_1(GASA)_1(DMA)_2 + GASA$	3.73×10^{-3}
$(SA)_1(GASA)_2(DMA)_2 \rightarrow (SA)_1(GASA)_1(DMA)_1 + (GASA)_1(DMA)_1$	6.35×10^{-15}
$(GASA)_3(DMA)_2 \rightarrow (GASA)_3(DMA)_1 + DMA$	5.28×10^{-13}
$(GASA)_3(DMA)_2 \rightarrow (GASA)_2(DMA)_2 + GASA$	1.09×10^{6}
$(GASA)_3(DMA)_2 \rightarrow (GASA)_2(DMA)_1 + (GASA)_1(DMA)_1$	5.25×10^{-21}
$(SA)_2(GASA)_1(DMA)_3 \rightarrow (SA)_2(GASA)_1(DMA)_2 + DMA$	2.38×10^{-5}
$(SA)_2(GASA)_1(DMA)_3 \rightarrow (SA)_1(GASA)_1(DMA)_2 + (SA)_1(DMA)_1$	4.92×10^{-10}
$(SA)_2(GASA)_1(DMA)_3 \rightarrow (GASA)_1(DMA)_1 + (SA)_2(DMA)_2$	1.08×10^{-18}
$(SA)_1(GASA)_2(DMA)_3 \rightarrow (SA)_1(GASA)_2(DMA)_2 + DMA$	6.15×10^{-8}
$(SA)_1(GASA)_2(DMA)_3 \rightarrow (GASA)_2(DMA)_2 + (SA)_1(DMA)_1$	2.76×10^{-1}
$(SA)_1(GASA)_2(DMA)_3 \rightarrow (SA)_1(GASA)_1(DMA)_2 + (GASA)_1(DMA)_1$	3.02×10^{-18}
$(GASA)_3(DMA)_3 \rightarrow (GASA)_3(DMA)_2 + DMA$	6.62×10^{-13}
$(GASA)_3(DMA)_3 \rightarrow (GASA)_2(DMA)_2 + (GPASA)_1(DMA)_1$	9.16×10^{-15}

Supporting information

Reference

Anttila, T., Kerminen, V.-M., and Lehtinen, K. E. J.: Parameterizing the formation rate of new particles: The effect of nuclei self-coagulation, J. Aerosol Sci., 41, 621-636, https://doi.org/10.1016/j.jaerosci.2010.04.008, 2010.

Kulmala, M., Petäjä, T., Nieminen, T., Sipilä, M., Manninen, H. E., Lehtipalo, K., Dal Maso, M., Aalto, P. P., Junninen, H., Paasonen, P., Riipinen, I., Lehtinen, K. E. J., Laaksonen, A., and Kerminen, V.-M.: Measurement of the nucleation of atmospheric aerosol particles, Nat. Protoc., 7, 1651-1667, https://doi.org/10.1038/nprot.2012.091, 2012.

Lehtinen, K. E. J., Dal Maso, M., Kulmala, M., and Kerminen, V.-M.: Estimating nucleation rates from apparent particle formation rates and vice versa: Revised formulation of the Kerminen–Kulmala equation, J. Aerosol Sci., 38, 988-994, https://doi.org/10.1016/j.jaerosci.2007.06.009, 2007.

Liu, L., Yu, F., Du, L., Yang, Z., Francisco, J. S., and Zhang, X.: Rapid sulfuric acid–dimethylamine nucleation enhanced by nitric acid in polluted regions, Proc. Natl. Acad. Sci. U.S.A., 118, e2108384118, https://doi.org/10.1073/pnas.2108384118, 2021.

Maso, M. D., Hyvärinen, A., Komppula, M., Tunved, P., Kerminen, V.-M., Lihavainen, H., Öviisanen, Y., Hansson, H.-C., and Kulmala, M.: Annual and interannual variation in boreal forest aerosol particle number and volume concentration and their connection to particle formation, Tellus B, 60, 495-508, https://doi.org/10.1111/j.1600-0889.2008.00366.x, 2008.

Olenius, T., Kupiainen-Määttä, O., Ortega, I., Kurtén, T., and Vehkamäki, H.: Free energy barrier in the growth of sulfuric acid–ammonia and sulfuric acid–dimethylamine clusters, J. Chem. Phys., 139, 084312, https://doi.org/10.1063/1.4819024, 2013.

Renard, J. J.; Calidonna, S. E.; Henley, M. V., Fate of ammonia in the atmosphere—a review for applicability to hazardous releases. J. Hazard. Mater. 108, 29-60, https://doi.org/10.1016/j.jhazmat.2004.01.015, 2004.

Riipinen, I., Sihto, S. L., Kulmala, M., Arnold, F., Dal Maso, M., Birmili, W., Saarnio, K., Teinilä, K., Kerminen, V. M., Laaksonen, A., and Lehtinen, K. E. J.: Connections between atmospheric sulphuric acid and new particle formation during QUEST III–IV campaigns in Heidelberg and Hyytiälä, Atmos. Chem.

Phys., 7, 1899-1914, https://doi.org/10.5194/acp-7-1899-2007, 2007.

Tan, S., Zhang, X., Lian, Y., Chen, X., Yin, S., Du, L., and Ge, M.: OH group orientation leads to organosulfate formation at the liquid aerosol surface, J. Am. Chem. Soc., 144, 16953-16964, https://doi.org/10.1021/jacs.2c05807, 2022.

Xia, D., Chen, J., Yu, H., Xie, H.-b., Wang, Y., Wang, Z., Xu, T., and Allen, D. T.: Formation Mechanisms of Iodine–Ammonia Clusters in Polluted Coastal Areas Unveiled by Thermodynamics and Kinetic Simulations, Environ. Sci. Technol., 54, 9235-9242, https://doi.org/10.1021/acs.est.9b07476, 2020.

Zhang, H., Kupiainen-Määttä, O., Zhang, X., Molinero, V., Zhang, Y., and Li, Z.: The enhancement mechanism of glycolic acid on the formation of atmospheric sulfuric acid–ammonia molecular clusters, J. Chem. Phys. 146, https://doi.org/10.1063/1.4982929, 2017.